ACES Asian Chemical Editorial Society

DOI: 10.1002/asia.201700204

CHEMISTRY AN ASIAN JOURNAL Full Paper

Diazaporphyrin Dimers

Nitrogen-Bridged Metallodiazaporphyrin Dimers: Synergistic Effects of Nitrogen Bridges and *meso*-Nitrogen Atoms on Structure and Properties

Masahiro Kawamata,[a] Takuma Sugai,[a] Mao Minoura,[b] Yasuhisa Maruyama,[c] Ko Furukawa,[d] Cole Holstrom,[e] Victor N. Nemykin,*[e, f] Haruyuki Nakano,[g] and Yoshihiro Matano*[a]

Abstract: NH-bridged and pyrazine-fused metallodiazaporphyrin dimers have been prepared from nickel(II) and copper(II) complexes of 3-amino-5,15-diazaporphyrin by Pd-catalyzed C–N cross-coupling and oxidative dimerization reactions, respectively. The synergistic effects of the nitrogen bridges and *meso*-nitrogen atoms play major roles in enhancing the light-harvesting properties and delocalization of an electron spin over the entire π-skeletons of the metallodiazaporphyrin dimers.

Introduction

Covalently linked porphyrin dimers (diporphyrins) have been extensively studied not only as artificial models for the special pair in photosynthetic reaction centers but also as functional dyes for materials science.[1] It is important to understand the intrinsic effects of the spacers and linkage patterns of diporphyrin π-systems on their optical, electrochemical and magnetic properties because such information is indispensable for the development of porphyrin-based materials. In the last decade, several research groups have explored nitrogen-based intervening spacers to diversify the inherent properties of diporphyrins.[2–13] For example, Arnold and co-workers reported the first example of a diporphyrin with an NH bridge (diporphyrinylamine) **P1** (Figure 1), which showed a split Soret band, indicating that excitonic coupling occurred between the two por-

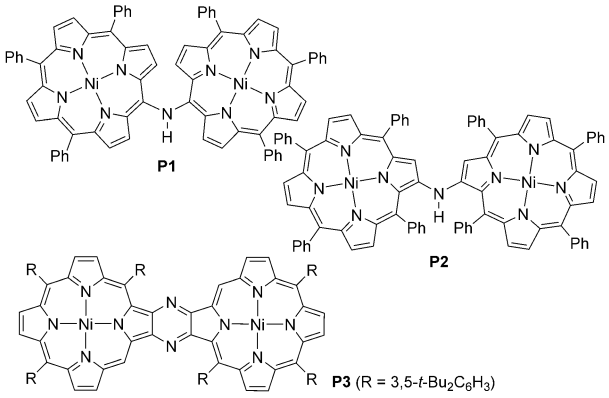

Figure 1. Diporphyrinylamines **P1** and **P2**, and pyrazine-fused diporphyrin **P3**.

[a] *M. Kawamata, T. Sugai, Prof. Dr. Y. Matano*
Department of Chemistry, Faculty of Science
Niigata University
Nishi-ku, Niigata 950-2181 (Japan)
E-mail: matano@chem.sc.niigata-u.ac.jp

[b] *Prof. Dr. M. Minoura*
Department of Chemistry, College of Science
Rikkyo University
Toshima-ku, Tokyo 171-8501 (Japan)

[c] *Y. Maruyama*
Department of Fundamental Sciences
Graduate School of Science and Technology
Niigata University
Nishi-ku, Niigata 950–2181 (Japan)

[d] *Prof. Dr. K. Furukawa*
Center for Instrumental Analysis
Institute for Research Promotion
Niigata University
Nishi-ku, Niigata 950–2181 (Japan)

[e] *C. Holstrom, Prof. Dr. V. N. Nemykin*
Department of Chemistry and Biochemistry
University of Minnesota Duluth
Duluth, Minnesota 55812-2496 (USA)
E-mail: vnemykin@d.umn.edu

[f] *Prof. Dr. V. N. Nemykin*
Department of Chemistry
University of Manitoba
Winnipeg MB, R3T 2N2 (Canada)
E-mail: Victor.Nemykin@umanitoba.ca

[g] *Prof. Dr. H. Nakano*
Department of Chemistry
Graduate School of Science
Kyushu University
Nishi-ku, Fukuoka 819-0395 (Japan)

Supporting information and the ORCID identification number(s) for the author(s) of this article can be found under http://dx.doi.org/10.1002/asia.201700204.

phyrin rings.[2] Ruppert and co-workers studied the effects of the intervening NH bridge on the fundamental properties of three different types of diporphyrinylamines including **P1** and **P2** (Figure 1).[6,7] Most of these diporphyrinylamines contained two porphyrin rings that were considerably twisted at the NH bridge because of the steric repulsion between the peripheral (*meso*/β) substituents. As a consequence, the two porphyrin rings in **P1** and **P2** were not effectively conjugated. Recently, Shinokubo et al. reported the pyrazine-fused diporphyrin **P3** and related compounds,[12,13] which showed twisted π-skeletons. Until recently, very little attention has been paid to nitrogen-bridged azaporphyrin dimers.

5,15-Diazaporphyrin (DAP) contains a π-system with intrinsic D_{2h} symmetry, which leads to an intense electronic transition from the HOMO to the LUMO at a longer wavelength than that of porphyrin.[14–16] Recently, we reported several examples of covalently linked metallo-DAP dimers (bisMDAPs) without a spacer or with an acetylene, butadiyne, or heterole spacer.[17,18] The optical properties of these bisMDAPs vary considerably depending on the intervening spacer. We envisioned that nitrogen bridges could also construct highly π-conjugated bisMDAPs because (i) nitrogen is the smallest unit that allows two DAP rings to be held in close proximity, (ii) the *p*-orbital of nitrogen can be involved in the conjugation with the adjacent DAP π-orbital, and (iii) the NH bridge can be used as a hydrogen-bond donor towards the *meso* nitrogen atoms of DAP. Herein, we report the first examples of NH-bridged and pyrazine-fused bisMDAPs, as well as their precursors β-nitro- and β-amino-substituted MDAPs. The synergistic effects of the nitrogen bridges and the *meso*-nitrogen atoms on the structures and optical, electrochemical, and magnetic properties of the bisMDAPs are investigated.

Results and Discussion

Scheme 1 outlines the synthesis of NH-bridged and pyrazine-fused bisNiDAPs. Treatment of NiDAP **1Ni**[19,20] with copper(II) nitrate in acetic anhydride and CH_2Cl_2 gave 3-nitro-NiDAP **2Ni**. Reduction of **2Ni** with $SnCl_2$/HCl afforded 3-amino-NiDAP **3Ni**. The C–N cross-coupling reaction of **3Ni** with 3-bromo-NiDAP **4Ni** under standard Buchwald–Hartwig conditions ($Pd(OAc)_2$, 2,2′-bis(diphenylphosphino)-1,1′-binaphthyl (*rac*-BINAP), and *t*BuONa)[21] afforded NH-bridged bisNiDAP **5Ni** as a black solid in 53% yield.

The pyrazine-fused bisNiDAP **6** was prepared by oxidative dimerization of **3Ni** using 2,3-dichloro-4,5-dicyano-1,4-benzoquinone (DDQ) as an oxidant based on Shinokubo's protocol for the synthesis of **P2**. In contrast, treatment of **3Ni** with *meta*-chloroperbenzoic acid (*m*CPBA) resulted in the oxidative reconstruction of its pyrrole ring to give diazaporpholactone **7** as the major product. This type of peripheral reconstruction from a β-aminoporphyrin was reported by Crossley in 1984.[22] The NH-bridged bisCuDAP **5Cu** was prepared from **1Cu** according to a similar procedure to that used to synthesize **5Ni**.

New compounds **2M**, **3M**, **5M**, **6**, and **7** were characterized by NMR spectroscopy, HRMS, and/or X-ray crystallography. The ^{1}H NMR spectra of **2Ni** and **3Ni** in $CDCl_3$ (Figure S1 a) exhibited

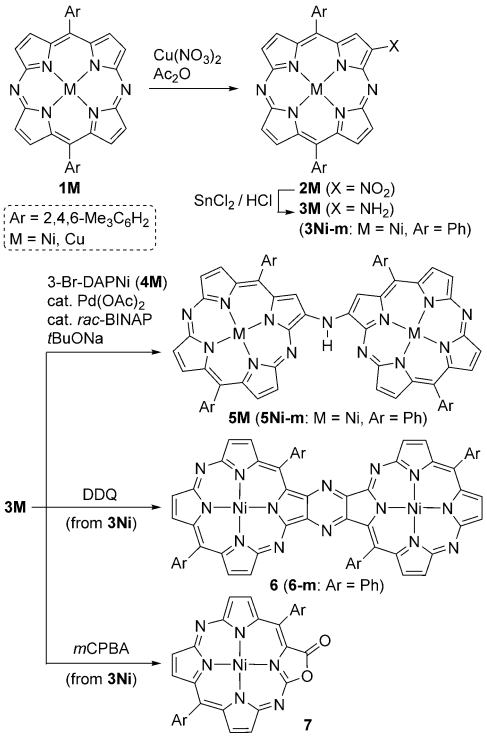

Scheme 1. Synthesis of **2M**, **3M**, **5M**, **6** and **7**; structures of models **3Ni-m**, **5Ni-m**, and **6-m** for DFT calculations. **4M**: Metal complexes of 3-bromo-10,20-dimesityl-5,15-diazaporphyrins. **1Ni**-**5Ni**: M = Ni; **1Cu**-**5Cu**: M = Cu.

singlet peaks at δ 9.30 and 7.36 ppm, respectively, which were assigned to the β_2-pyrrolic protons adjacent to the nitro and amino groups, respectively. The ^{1}H NMR spectrum of **5Ni** in $CDCl_3$ (Figure S1 b) showed only one set of DAP-derived protons (one singlet originating from the β_2 proton and three sets of doublets from the other peripheral β protons), indicating that **5Ni** had C_2 or C_s symmetry on average. The NH proton of **5Ni** (δ = 11.90 ppm) was shifted downfield compared to the NH_2 proton of **3Ni** (δ = 5.89 ppm) and the NH proton of **P1** (δ = 6.16 ppm; in $C_2D_2Cl_4$, at 100 °C). This relatively large downfield shift could be attributed not only to the ring-current effects of the neighboring DAP rings but also the intramolecular hydrogen-bonding interaction with the adjacent *meso* nitrogen atoms. The ^{1}H NMR spectrum of **7** displayed three sets of doublets attributable to six β protons.

The structure of **5Ni** was unambiguously elucidated by XRD analysis.[23] As illustrated in Figure 2, the two DAP rings and NH bridge were on the same plane with a H-N7-C3-C4 torsion angle of 3.4°, and the DAP π-planes were almost flat like that of **1Ni**. From the viewpoint of molecular geometry, the two DAP π-systems in **5Ni** were more effectively conjugated through the NH bridge than the two porphyrin π-systems in Arnold's **P1** where the porphyrin rings displayed a large twist angle because of steric congestion.[2] The distance between the NH hydrogen and *meso* nitrogen (N5) atoms in **5Ni** was 2.32 Å, which was considerably shorter than the sum of their van der Waals radii (2.75 Å). This implies that a hydrogen-bonding interaction between these two atoms plays a pivotal role in the formation of coplanar structure, as suggested from its

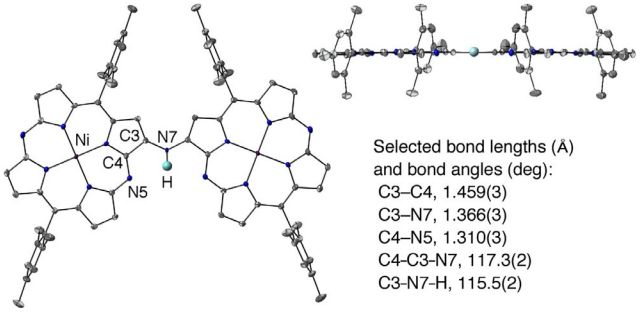

Figure 2. Top and side views for **5Ni** (50% probability ellipsoids). Hydrogen atoms (except for NH) and solvent molecules are omitted for clarity.

^{1}H NMR spectrum in solution. The crystal structure of **6** was also elucidated (Figure S2, Supporting Information), although the crystallographic data could not be fully refined to a satisfactory level because of uncertain loss of solvent molecules included in the crystal. The pyrazine ring in **6** was completely planar, whereas each NiDAP ring was slightly ruffled. As a consequence, the whole π-plane of **6** was twisted like that of Shinokubo's **P3**; however, the twist angle between the pyrazine and pyrrole rings in **6** (27.0°) was appreciably smaller than that of **P3** (40.8°), reflecting the difference in flexibility of the NiDAP and Ni-porphyrin rings. The structure of **7** was also confirmed by X-ray crystallography (Figure S2).

The optical properties of the new DAP derivatives were studied by UV/Vis absorption spectroscopy. As shown in Figure 3a, the substitution of the β_3 proton with a nitro/amino group (from **1Ni** to **2Ni**/**3Ni**) caused substantial bathochromic shifts of the Q band of the NiDAP π-system, reflecting the electronic effects of these functional groups (see below). The absorption spectrum of NH-bridged bisNiDAP **5Ni** contained multiple peaks at wavelengths longer than 500 nm. It is noteworthy that the longest-wavelength absorption bands of **5Ni** (λ_{max} = 706 nm, log ε = 5.0) and **6** (λ_{max} = 647 nm, log ε = 5.1) were red-shifted and more intense than those of **P2** (λ_{max} = 626 nm, log ε = 4.6) and **P3** (λ_{max} = 628 nm, log ε = 4.7), respectively. These data imply that linking two DAP units with nitrogen is a highly promising strategy to develop new azaporphyrin-based sensitizers with broad absorption spectra reaching the near-infrared (NIR) region. The copper complexes **2Cu**, **3Cu**, and **5Cu** exhibited similar spectral features (Figure 3c).

To gain deeper insight into the origin of the excited states of the DAP π-systems, we performed time-dependent DFT (TD-DFT) calculations on models **3Ni-m**, **5Ni-m** and **6-m**, and magnetic circular dichroism (MCD) measurements on **3Ni** and **5Ni**. The results of the TD-DFT calculations qualitatively support the observed spectral features (Tables S1, S2 and Figures S4–S7). The lowest-energy excitation for each model was dominated by a HOMO-to-LUMO transition. As shown in Figures S4 and S5, the HOMOs of **3Ni-m** and **5Ni-m** were partially distributed on their amino groups, whereas the LUMOs were essentially localized on the DAP rings. The MCD spectra of **3Ni** and **5Ni** exhibited broad signals at 600–670 and 630–750 nm, respectively (Figure 3b), corresponding to the broad absorptions in the same regions. These results indicated that the HOMO-to-LUMO

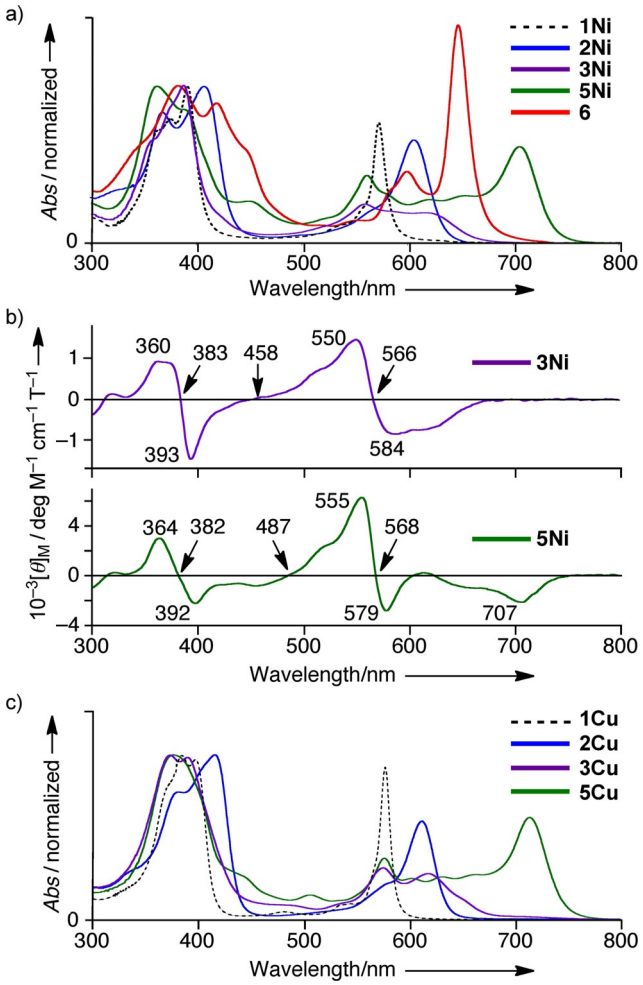

Figure 3. a) UV/Vis absorption spectra of **1Ni**, **2Ni**, **3Ni**, **5Ni**, and **6** in CH_2Cl_2. b) MCD spectra of **3Ni** and **5Ni** in CH_2Cl_2. c) UV/Vis absorption spectra of **1Cu**, **2Cu**, **3Cu**, and **5Cu** in CH_2Cl_2.

transitions of **3Ni** and **5Ni** had a substantial charge-transfer character from NH_2/NH (donor) to DAP (acceptor) units. Furthermore, the strong minus-to-plus MCD signals at 540–580 nm (Figure 3b), as well as the theoretically calculated results indicated that the intense absorption bands at λ_{max} 560 nm (for **3Ni**) and 561 nm (for **5Ni**) could be attributed to the DAP-based π–π* transitions. The TD-DFT calculations of **6-m** revealed that the absorption band at λ_{max} 647 nm for **6** stemmed from DAP-based π–π* transitions.

Redox potentials of the MDAPs were measured in CH_2Cl_2 with Bu_4NPF_6 as the supporting electrolyte (Figure S8). The oxidation and reduction potentials (E_{ox} and E_{red}, respectively, versus ferrocene/ferrocenium) of the MDAPs are listed in Table 1. The E_{ox} and E_{red} values of **2M** were shifted anodically, whereas those of **3M** were shifted cathodically relative to the respective values of **1M**. These shifts reflected typical resonance effects of the electron-withdrawing nitro group and electron-donating amino group at their periphery. The E_{ox1} and E_{red1} values of **5Ni** (+0.41 and −1.48 V) and **6** (+0.72 and −1.25 V) were more positive than the corresponding values of **P2** (+0.27 and −1.76 V) and **P3** (+0.488 and −1.58 V), reflect-

Table 1. Optical and electrochemical data for DAPs measured in CH_2Cl_2.

DAP	λ_{max} [nm] (log ε) [a]	E_{ox} [V][b]	E_{red} [V][b]	ΔE [V][c]
1Ni[d]	571 (4.8)	+0.80	−1.40, −2.02	2.20
1Cu[d]	577 (4.9)	+0.77	−1.37, −1.95	2.14
2Ni	606 (4.5)	+1.04	−1.01, −1.35, −1.93	2.05
2Cu	612 (4.5)	+1.01	−0.97, −1.29	1.98
3Ni	560 (4.2), 614 (4.1)	+0.40,[e] +0.79	−1.50, −1.96	1.90
3Cu	574 (4.4), 619 (4.3)	+0.37,[e] +0.76	−1.46, −1.86	1.83
5Ni	561 (4.8), 706 (5.0)	+0.41, +0.66	−1.37, −1.48, −1.93	1.78
5Cu	568 (4.7), 702 (5.0)	+0.40, +0.66	−1.33, −1.48, −1.86	1.73
6	598 (4.6), 647 (5.1)	+0.72, +0.96	−1.25, −1.42, −1.84, −1.98	1.97
7	618 (4.8)	+0.88	−1.10, −1.66	1.98

[a] Absorption maxima (>500 nm, log ε>4). [b] Oxidation (E_{ox}) and reduction (E_{red}) potentials versus Fc/Fc^+. The redox processes were reversible unless otherwise noted. [c] $\Delta E = E_{ox1} - E_{red1}$. [d] From ref. [19]. [e] Irreversible.

ing the intrinsic difference in the redox properties of DAP and porphyrin. The large splitting energies between the first and second redox processes of **5M** (E_{ox2}–E_{ox1} = 0.25–0.26 V) and **6** (E_{ox2}–E_{ox1} = 0.24 V; E_{red1}–E_{red2} = 0.17 V) indicated that an unpaired electron spin in the singly oxidized/reduced species of **5M** and **6** would be effectively delocalized over the two DAP π-frameworks through the spacers.

The E_{ox1} values of **5M** were almost identical to those of **3M**, suggesting that the first oxidation of **5M** took place at the bridging nitrogen atom. The radical cation of **5Ni** (**5Ni**$^{\cdot+}$), generated by chemical or electrochemical oxidation of **5Ni** in CH_2Cl_2, showed broad absorption bands with λ_{max} of 605 and 800 nm (Figure S9). The oxidized species **5Ni**$^{\cdot+}$ was further studied by EPR spectroscopy. An EPR signal of **5Ni**$^{\cdot+}$ was detected at g = 2.0088 with the fine structure derived from the ^{14}N and ^{1}H nuclei (Figure S10). The hyperfine coupling constants of **5Ni**$^{\cdot+}$ (A_N = 5.7 G, A_H = 4.3 G) were comparable to those of a radical cation of **P2** (A_N = 4.8 G, A_H = 5.2 G)[6] and consistent with the theoretically calculated spin density distribution of radical model **5Ni-m**$^{\cdot+}$. It should be noted that the first oxidation process of **5Ni** was reversible, whereas that of **3Ni** was irreversible. These results highlighted that the N-centered radical cation **5Ni**$^{\cdot+}$ was stabilized by an effective delocalization of the electron spin over the two coplanar NiDAP rings.

To understand the exchange interaction between the two copper(II) spins in **5Cu**, we also measured its EPR spectrum in 2-methyltetrahydrofuran (2-MeTHF) at 45 K (Figure 4). The observed spectrum was fully simulated as two magnetically coupled CuDAPs, implying that the electron spins at the copper(II) centers would effectively interact with each other through the NH bridge (for the EPR spectrum of **1Cu**, see Figure S11 in the Supporting Information). Based on the point dipole approximation, the estimated Cu···Cu distance in **5Cu** was 10.4 Å from the D value of the spin Hamiltonian parameters. This value was close to the Ni···Ni distance in **5Ni** (10.6 Å), implying that **5Cu** had a flat π-plane with the N–H···N hydrogen bonds such as those in **5Ni**.

Conclusions

We prepared NH-bridged and pyrazine-fused bisMDAPs and investigated their structures and optical, electrochemical, and magnetic properties by X-ray crystallography, various spectroscopies, and DFT calculations. The NH-bridged bisNiDAP had a highly flat π-plane because of the presence of cooperative N–H···N(*meso*) hydrogen bonds. The UV/Vis absorption spectra of the new bisMDAPs displayed intense absorption bands extending to the NIR region. All the data obtained for the paramagnetic species indicated there was effective electron-spin communication between the two DAP π-systems through the nitrogen bridges. The synergistic effects of the nitrogen bridges and *meso*-nitrogen atoms play important roles in harvesting a wide range of visible light and delocalization of an unpaired electron spin over the entire π-skeletons of the DAPs. Further studies on the structural modification of the present DAPs aiming to provide NIR-responsive dyes are now underway.

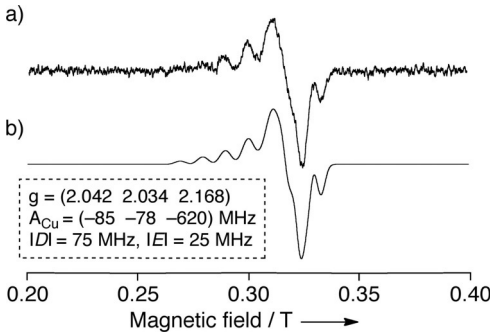

Figure 4. EPR spectra of **5Cu**: a) Observed in 2-MeTHF at 45 K. b) Simulated.

Experimental Section

All melting points were recorded on a Yazawa micro melting point apparatus and are uncorrected. The identity and purity of the prepared compounds were analyzed by ^{1}H (400 MHz or 700 MHz) NMR spectroscopy (Varian 400 MHz and 700 MHz spectrometers) and high-resolution mass spectrometry (Thermo Fisher Scientific EXACTIVE spectrometer; electron spray-quadrupole). The ^{1}H chemical shifts are reported in ppm as relative values versus tetramethylsilane (in $CDCl_3$ and CD_2Cl_2). The IR spectra were measured on a PerkinElmer Spectrum GX spectrometer using KBr pellets. UV/Vis absorption spectra were measured at room temperature on a JASCO V-530 or V-670 spectrometer. Electrochemical measurements (cyclic voltammetry and differential pulse voltammetry) were performed at room temperature on a CH Instruments model 650E electrochemical workstation using a glassy carbon working electrode, a platinum wire counter electrode, and an Ag/Ag^+ [0.01 M $AgNO_3$, 0.1 M Bu_4NPF_6 (MeCN)] reference electrode. MDAP **1M**[19] and 3-bromo-MDAP **4M**[17] (M = Ni, Cu) were prepared according to their reported procedures. Other chemicals and solvents were of reagent grade quality and used without further purification unless otherwise noted. Thin-layer chromatography was per-

formed on Kieselgel 60 F254, and preparative column chromatography was performed using Silica Gel 60, spherical, neutrality. All reactions were performed under an argon or nitrogen atmosphere.

Synthesis and Characterization

2M: Copper(II) nitrate (84.3 mg, 0.35 mmol) was added to acetic anhydride (2.0 mL), and the mixture was stirred for 10 min at room temperature. The resulting suspension was added to a CH_2Cl_2 solution (30 mL) of **1Ni** (104.6 mg, 0.17 mmol), and the mixture was stirred for 38 h at room temperature. The mixture was then neutralized by adding an aqueous NaOH solution (10%), washed with water, and concentrated under reduced pressure. The residue was subjected to column chromatography on silica gel (hexane/AcOEt = 10:1). Compound **2Ni** (R_f = 0.44) was isolated as a dark purple solid (98.0 mg, 89%) by reprecipitation from CH_2Cl_2/MeOH. According to a similar procedure, **2Cu** (R_f = 0.24; hexane/AcOEt = 10:1) was prepared in 57% yield from **1Cu. 2Ni**: m.p. > 300 °C; ^{1}H NMR (700 MHz, CD_2Cl_2): δ = 1.81 (s, 12H, *ortho*-Me), 2.60 (s, 3H, *para*-Me), 2.62 (s, 3H, *para*-Me), 7.27 (s, 2H, *meta*-H), 7.28 (s, 2H, *meta*-H), 8.74 (d, J = 4.9 Hz, 1H, pyrrole-β), 8.76 (d, J = 4.9 Hz, 1H, pyrrole-β), 8.77 (d, J = 4.9 Hz, 1H, pyrrole-β), 9.08 (d, J = 4.9 Hz, 1H, pyrrole-β), 9.13 (d, J = 4.9 Hz, 1H, pyrrole-β), 9.26 (d, J = 4.9 Hz, 1H, pyrrole-β), 9.30 ppm (s, 1H, pyrrole-β); UV/Vis (CH_2Cl_2): λ_{max} (ε) = 368 (44000), 407 (53000), 606 nm (35000 $M^{-1}cm^{-1}$); HRMS (ESI): *m/z* calcd for $C_{36}H_{29}N_7NiO_2$: 650.1809; found: 650.1803 $[M+H]^+$. **2Cu**: M.p. > 300 °C; UV/Vis (CH_2Cl_2): λ_{max} (ε) = 380 (41000), 415 (52000), 612 nm (31000 $M^{-1}cm^{-1}$); HRMS (ESI): *m/z* calcd for $C_{36}H_{30}CuN_7O_2$: 655.1752; found: 655.1732 $[M+H]^+$.

3M: A mixture of **2Ni** (40.5 mg, 0.062 mmol), $SnCl_2{\cdot}2H_2O$ (75.2 mg, 0.33 mmol), 3 M HCl (1.1 mL), and CH_2Cl_2 (25 mL) was heated under reflux conditions for 0.5 h. The mixture was then neutralized by adding an aqueous NaOH solution (10%), washed with water, and concentrated under reduced pressure. The residue was subjected to column chromatography on silica gel (hexane/AcOEt = 7:1). Compound **3Ni** (R_f = 0.41; hexane/AcOEt = 5:1) was isolated as a purple solid (31.3 mg, 82%) by reprecipitation from CH_2Cl_2/MeOH. According to a similar procedure, **3Cu** (R_f = 0.52; hexane/AcOEt = 5:1) was prepared in 57% yield from **2Cu. 3Ni**: m.p. > 300 °C; ^{1}H NMR (700 MHz, $CDCl_3$): δ = 1.80 (s, 6H, *ortho*-Me), 1.82 (s, 6H, *ortho*-Me), 2.59 (s, 3H, *para*-Me), 2.60 (s, 3H, *para*-Me), 5.89 (s, 2H, NH_2), 7.24 (s, 2H, *meta*-H), 7.25 (s, 2H, *meta*-H), 7.36 (s, 1H, pyrrole-β), 8.64 (d, J = 4.3 Hz, 1H, pyrrole-β), 8.70 (d, J = 4.3 Hz, 2H, pyrrole-β), 8.98 (d, J = 4.3 Hz, 1H, pyrrole-β), 9.03 (d, J = 4.3 Hz, 1H, pyrrole-β), 9.05 ppm (d, J = 4.3 Hz, 1H, pyrrole-β); λ_{max} (ε) = 387 (64000), 560 (16000), 614 nm (12000 $M^{-1}cm^{-1}$); HRMS (ESI): *m/z* calcd for $C_{36}H_{32}N_7Ni$: 620.2067; found: 620.2061 $[M+H]^+$. **3Cu**: M.p. > 300 °C; UV/Vis (CH_2Cl_2): λ_{max} (ε) = 373 (68000), 390 (70000), 574 (23000), 616 nm (19000 $M^{-1}cm^{-1}$); HRMS (ESI): *m/z* calcd for $C_{36}H_{32}CuN_7$: 625.2010; found: 625.1990 $[M+H]^+$.

5M: A mixture of **3Ni** (18.4 mg, 0.030 mmol), **4Ni** (16.6 mg, 0.024 mmol), $Pd(OAc)_2$ (1.6 mg, 0.008 mmol), *rac*-BINAP (3.5 mg, 0.006 mmol), *t*BuONa (3.5 mg, 0.072 mmol) and toluene (10 mL) was heated under reflux conditions for 6 h. After being cooled, the mixture was washed with water and concentrated under reduced pressure. The residue was subjected to column chromatography on silica gel (hexane/AcOEt = 10:1). Compound **5Ni** (R_f = 0.41; hexane/AcOEt = 5:1) was isolated as a black solid (15.7 mg, 53%) by reprecipitation from CH_2Cl_2/MeOH. According to a similar procedure, **5Cu** (R_f = 0.42; hexane/AcOEt = 5:1) was prepared in 36% yield from **3Cu** and **4Cu. 5Ni**: m.p. > 300 °C; ^{1}H NMR (700 MHz, $CDCl_3$): δ = 1.87 (s, 12H, *ortho*-Me), 1.89 (s, 12H, *ortho*-Me), 2.63 (s, 6H, *para*-Me), 2.83 (s, 6H, *para*-Me), 7.29 (s, 4H, *meta*-H), 7.34 (s, 4H, *meta*-H), 8.19 (s, 2H, pyrrole-β), 8.73 (d, J = 4.6 Hz, 2H, pyrrole-β), 8.75 (d, J = 4.6 Hz, 2H, pyrrole-β), 8.84 (d, J = 4.6 Hz, 2H, pyrrole-β), 9.09 (d, J = 4.6 Hz, 2H, pyrrole-β), 9.12 (d, J = 4.6 Hz, 2H, pyrrole-β), 9.38 (d, J = 4.6 Hz, 2H, pyrrole-β), 11.90 ppm (s, 1H, NH); UV/Vis (CH_2Cl_2): λ_{max} (ε) = 362 (150000), 387 (130000), 561 (65000), 706 nm (93000 $M^{-1}cm^{-1}$); HRMS (ESI): *m/z* calcd for $C_{72}H_{60}N_{13}Ni_2$: 1222.3796; found: 1222.3799 $[M]^+$. **5Cu**: m.p. > 300 °C; UV/Vis (CH_2Cl_2): λ_{max} (ε) = 374 (152000), 568 (56000), 702 nm (94000 $M^{-1}cm^{-1}$); HRMS (ESI): *m/z* calcd for $C_{72}H_{60}Cu_2N_{13}$: 1232.3681; found: 1232.3661$[M+H]^+$.

6: A mixture of **3Ni** (13.9 mg, 0.022 mmol), DDQ (32.9 mg, 0.14 mmol), and $CHCl_3$ (20 mL) was stirred for 20 h at room temperature. The mixture was then concentrated under reduced pressure, and the residue was subjected to column chromatography on silica gel (hexane/AcOEt = 7:1). Compound **6** was isolated as a dark purple solid (2.7 mg, 20%) by reprecipitation from CH_2Cl_2/MeOH. m.p. > 300 °C; ^{1}H NMR (700 MHz, $CDCl_3$): δ = 1.86 (s, 12H, *ortho*-Me), 1.89 (s, 12H, *ortho*-Me), 2.64 (s, 6H, *para*-Me), 3.12 (s, 6H, *para*-Me), 7.30 (s, 4H, *meta*-H), 7.66 (s, 4H, *meta*-H), 8.80 (d, J = 5.0 Hz, 2H, pyrrole-β), 8.89 (d, J = 5.0 Hz, 2H, pyrrole-β), 9.11 (d, J = 5.0 Hz, 2H, pyrrole-β), 9.18 (d, J = 5.0 Hz, 2H, pyrrole-β), 9.24 (d, J = 5.0 Hz, 2H, pyrrole-β), 9.25 ppm (d, J = 5.0 Hz, 2H, pyrrole-β); λ_{max} (ε) = 381 (92000), 417 (82000), 598 (41000), 647 nm (127000 $M^{-1}cm^{-1}$); HRMS (ESI): *m/z* calcd for $C_{72}H_{57}N_{14}Ni_2$: 1233.3592; found: 1233.3573 $[M+H]^+$.

7: *m*CPBA (85.9 mg, 0.498 mmol) was added to a CH_2Cl_2 solution (20 mL) of **3Ni** (37.9 mg, 0.0611 mmol), and the mixture was stirred for 7 h at room temperature. The resulting mixture was neutralized by adding an aqueous NaOH solution (10%), washed with water, and concentrated under reduced pressure. The residue was subjected to column chromatography on silica gel (R_f = 0.45; hexane/AcOEt = 5:1). Compound **7** was isolated as a black solid (21.9 mg, 57%). m.p. > 300 °C; ^{1}H NMR (400 MHz, $CDCl_3$): δ = 1.82 (s, 12H, *ortho*-Me), 2.56 (s, 3H, *para*-Me), 2.58 (s, 3H, *para*-Me), 7.24 (s, 4H, *meta*-H), 8.45 (d, 1H, J = 4.8 Hz, pyrrole-β), 8.51 (d, 1H, J = 4.8 Hz, pyrrole-β), 8.59 (d, 1H, J = 4.8 Hz, pyrrole-β), 8.80 (d, 1H, J = 4.8 Hz, pyrrole-β), 8.96 (d, 1H, J = 4.6 Hz, pyrrole-β), 8.97 ppm (d, 1H, J = 4.6 Hz, pyrrole-β); λ_{max} (ε) = 349 (33000), 392 (40000), 618 nm (66000 $M^{-1}cm^{-1}$); IR (KBr): $\tilde{\nu}_{max}$ = 1783 cm^{-1} (C=O); HRMS (ESI): *m/z* calcd for $C_{35}H_{29}N_6NiO_2$: 623.1700; found: 623.1676 $[M+H]^+$.

Selected X-ray Crystallographic Data

5Ni: Molecular formula = $C_{80}H_{65}Cl_{16}N_{15}Ni_2$, molecular weight = 1921.09, 0.20×0.10×0.05 mm, orthorhombic, *Pnma*, a = 18.1957(8) Å, b = 38.5630(18) Å, c = 11.9954(6) Å, V = 8416.9(7) Å^3, Z = 4, ρ_{calcd} = 1.516 g cm^{-3}, μ = 10.10 cm^{-1}, collected 75905, independent 9798, parameters 585, R_w = 0.1173 (all data), $R1$ = 0.0477 ($I > 2.0\sigma(I)$), GOF = 1.102. CCDC 1528879.

The crystallographic data for **6** and **7** could not be fully refined to a satisfactory level because of uncertain loss of solvent molecules included in the crystal (for **6**) or positional disorder (for **7**). Regarding the positional disorder of **7**, the lactone part was located in each pyrrole ring crystallographically, with occupancies of the OCO unit of 0.2, 0.3, 0.2 and 0.3 at the rings.

DFT Calculations

The geometries of **3Ni-m**, **5Ni-m**, **6-m**, and **5Ni-m**$^{\cdot+}$ were optimized using the DFT method in which the solvent effect of CH_2Cl_2 was included by the polarizable continuum model (PCM).[24] The basis sets used were 6–311G(d,p) basis set[25] for H, C, and N and the Wachters–Hay all-electron basis set[26] supplemented with one

f-function (exponent: 1.29) for Ni. The functional of DFT was the Becke, three-parameter, Lee–Yang–Parr (B3LYP) exchange-correlation functional.[27] The Cartesian coordinates are summarized in Table S1. The excitation energies and oscillator strengths listed in Table S2 were computed with the TD-DFT method. All of the calculations were carried out using the Gaussian 09 suite of programs.[28] Selected Kohn–Sham orbitals and their energies are summarized in Figures S4–S6.

EPR Measurements

5Ni$^{\bullet+}$: A solution sample of **5Ni** (1 mM) and Bu_4NPF_6 (0.1 M) in CH_2Cl_2 in an electrolysis EPR cell with two electrodes was prepared. The electrolysis EPR spectra were recorded using a JEOL JES-FA200 spectrometer under a 3.6 V Matsusada Precision PL-18-5 current source at room temperature. Spectral simulation was performed using EasySpin,[29] a MATLAB toolbox. The selected spin-Hamiltonian parameters are summarized in Figure S10.

5Cu: A solution sample of **5Cu** in 2-methyltetrahydrofuran in a quartz EPR tube was degassed by repeated freeze/pump/thaw cycles and sealed under the vacuum by flame. The continuous-wave (cw) EPR spectra for **5Cu** were recorded using a JEOL JES-FA200 spectrometer equipped with an OXFORD ESR900 He-flow-type cryostat. The measurement temperature was controlled by an OXFORD Mercury temperature controller. The selected spin-Hamiltonian parameters are summarized in Figure S11.

Acknowledgements

This work was supported by JSPS KAKENHI (15H00931, 15K13762 to YM, 15H00962 to MM, and 24109008, 25287091 to KF, 15K05392 to HN). VNN would like to acknowledge support from the University of Manitoba, Minnesota Supercomputing Institute, and WestGrid.

Keywords: diazaporphyrins · EPR spectroscopy · macrocycles · porphyrins · transition metals

[1] N. Aratani, A. Osuka in *Handbook of Porphyrin Science, Vol. 1* (Eds.: K. M. Kadish, K. M. Smith, R. Guilard), World Scientific, New Jersey, **2010**, pp. 1–132.
[2] L. J. Esdaile, M. O. Senge, D. P. Arnold, *Chem. Commun.* **2006**, 4192.
[3] L. J. Esdaile, P. Jensen, J. C. McMurtrie, D. P. Arnold, *Angew. Chem. Int. Ed.* **2007**, *46*, 2090; *Angew. Chem.* **2007**, *119*, 2136.
[4] B. Bašić, J. C. McMurtrie, D. P. Arnold, *J. Porphyrins Phthalocyanines* **2010**, *14*, 481.
[5] S. R. Harper, M. C. Pfrunder, L. J. Esdaile, P. Jensen, J. C. McMurtrie, D. P. Arnold, *Eur. J. Org. Chem.* **2015**, 2807.
[6] A. M. V. M. Pereira, M. G. P. M. S. Neves, J. A. S. Cavaleiro, C. Jeandon, J.-P. Gisselbrecht, S. Choua, R. Ruppert, *Org. Lett.* **2011**, *13*, 4742.
[7] A. M. V. M. Pereira, C. Jeandon, J. A. S. Cavaleiro, M. G. P. M. S. Neves, R. Ruppert, *J. Porphyrins Phthalocyanines* **2014**, *18*, 727.
[8] C. H. Devillers, S. Hebié, D. Lucas, H. Cattey, S. Clément, S. Richeter, *J. Org. Chem.* **2014**, *79*, 6424.
[9] A. Tatar, B. Dolenský, H. Dvořáková, V. Král, *Tetrahedron Lett.* **2012**, *53*, 6015.
[10] T. Bruhn, F. Witterauf, D. C. G. Götz, C. T. Grimmer, M. Wurtemberger, U. Radius, G. Bringmann, *Chem. Eur. J.* **2014**, *20*, 3998.
[11] D.-M. Shen, C. Liu, X.-G. Chen, Q.-Y. Chen, *Synlett* **2009**, *6*, 945.
[12] M. Akita, S. Hiroto, H. Shinokubo, *Angew. Chem. Int. Ed.* **2012**, *51*, 2894; *Angew. Chem.* **2012**, *124*, 2948.
[13] S. Ito, S. Hiroto, S. Lee, M. Son, I. Hisaki, T. Yoshida, D. Kim, N. Kobayashi, H. Shinokubo, *J. Am. Chem. Soc.* **2015**, *137*, 142.
[14] N. Kobayashi in *The Porphyrin Handbook, Vol. 2* (Eds.: K. M. Kadish, K. M. Smith, R. Guilard), Academic Press, San Diego, **2000**, pp. 302–360.
[15] H. Ogata, T. Fukuda, K. Nakai, Y. Fujimura, S. Neya, P. A. Stuzhin, N. Kobayashi, *Eur. J. Inorg. Chem.* **2004**, 1621.
[16] Y. Matano, *Chem. Rev.* **2017**, *117*, 3138.
[17] Y. Matano, D. Fujii, T. Shibano, K. Furukawa, T. Higashino, H. Nakano, H. Imahori, *Chem. Eur. J.* **2014**, *20*, 3342.
[18] S. Omomo, Y. Maruyama, K. Furukawa, T. Furuyama, H. Nakano, N. Kobayashi, Y. Matano, *Chem. Eur. J.* **2015**, *21*, 2003.
[19] a) Y. Matano, T. Shibano, H. Nakano, H. Imahori, *Chem. Eur. J.* **2012**, *18*, 6208; b) Y. Matano, T. Shibano, H. Nakano, Y. Kimura, H. Imahori, *Inorg. Chem.* **2012**, *51*, 12879.
[20] M. Horie, Y. Hayashi, S. Yamaguchi, H. Shinokubo, *Chem. Eur. J.* **2012**, *18*, 5919.
[21] a) J. P. Wolfe, S. Wagaw, J.-F. Marcoux, S. L. Buchwald, *Acc. Chem. Res.* **1998**, *31*, 805; b) J. F. Hartwig, *Acc. Chem. Res.* **1998**, *31*, 852.
[22] M. J. Crossley, L. G. King, *J. Chem. Soc. Chem. Commun.* **1984**, 920.
[23] CCDC 1528879 contains the supplementary crystallographic data for this paper. These data can be obtained free of charge from The Cambridge Crystallographic Data Centre.
[24] E. T. Cancès, B. Mennucci, J. Tomasi, *J. Chem. Phys.* **1997**, *107*, 3032.
[25] R. Krishnan, J. S. Binkley, R. Seeger, J. A. Pople, *J. Chem. Phys.* **1980**, *72*, 650.
[26] a) A. J. H. Wachters, *J. Chem. Phys.* **1970**, *52*, 1033; b) P. J. Hay, *J. Chem. Phys.* **1977**, *66*, 4377; c) K. Raghavachari, G. W. Trucks, *J. Chem. Phys.* **1989**, *91*, 1062.
[27] a) A. D. Becke, *J. Chem. Phys.* **1993**, *98*, 5648; b) C. Lee, W. Yang, R. G. Parr, *Phys. Rev. B* **1988**, *37*, 785.
[28] Gaussian 09, Revision D.01, M. J. Frisch, G. W. Trucks, H. B. Schlegel, G. E. Scuseria, M. A. Robb, J. R. Cheeseman, G. Scalmani, V. Barone, B. Mennucci, G. A. Petersson, H. Nakatsuji, M. Caricato, X. Li, H. P. Hratchian, A. F. Izmaylov, J. Bloino, G. Zheng, J. L. Sonnenberg, M. Hada, M. Ehara, K. Toyota, R. Fukuda, J. Hasegawa, M. Ishida, T. Nakajima, Y. Honda, O. Kitao, H. Nakai, T. Vreven, J. A. Montgomery, Jr., J. E. Peralta, F. Ogliaro, M. Bearpark, J. J. Heyd, E. Brothers, K. N. Kudin, V. N. Staroverov, T. Keith, R. Kobayashi, J. Normand, K. Raghavachari, A. Rendell, J. C. Burant, S. S. Iyengar, J. Tomasi, M. Cossi, N. Rega, J. M. Millam, M. Klene, J. E. Knox, J. B. Cross, V. Bakken, C. Adamo, J. Jaramillo, R. Gomperts, R. E. Stratmann, O. Yazyev, A. J. Austin, R. Cammi, C. Pomelli, J. W. Ochterski, R. L. Martin, K. Morokuma, V. G. Zakrzewski, G. A. Voth, P. Salvador, J. J. Dannenberg, S. Dapprich, A. D. Daniels, Ö. Farkas, J. B. Foresman, J. V. Ortiz, J. Cioslowski, D. J. Fox, Gaussian, Inc., Wallingford CT, **2013**.
[29] S. Stoll, A. Schweiger, *J. Magn. Reson.* **2006**, *178*, 42.

Manuscript received: February 9, 2017
Accepted Article published: February 9, 2017
Final Article published: February 28, 2017